Mechanism of sulfonation-induced chain scission of selectively oxidized polysaccharides

Mechanism of sulfonation-induced chain scission of selectively oxidized polysaccharides

L. Munster, B. Hanulíková, M. Machovský, F. Latečka, I. Kuřitka, J. Vícha*

Centre of Polymer Systems, University Institute, Tomas Bata University in Zlin, tr. Tomase Bati 5678, 760 01, Zlín, Czech Republic

*Corresponding author. E-mail address: jvicha@utb.cz (J. Vícha).

ABSTRACT

Oxidation of polysaccharides to 2,3-dicarboxypolysaccharides is a two-stage process, where selective oxidation by periodate is followed by secondary oxidation by chlorite. Addition of sulfamic acid before the secondary oxidation influences the molecular weight and degree of oxidation of the product. Here, mechanism of sulfamic acid-catalysed chain scission is elucidated for selectively oxidized cellulose and dextrin. Initially, sulfamic acid sulfonates the aldehyde groups of 2,3-dialdehydepolysaccharide. Introduced -SO_3H groups are in ideal position to protonate the oxygen atom of 1-4' glycosidic bond and to trigger acidic hydrolysis. This can be used to obtain a direct control over the molecular weight of the product. Observed slightly lower degree of oxidation was ascribed to the ability of sulfamic acid to scavenge the hypochlorite and thus protect the intermolecular hemiacetals from oxidation. Usually undesirable hypochlorite thus seems to be necessary for preparation of selectively oxidized polysaccharides with degree of oxidation above 90%.

Keywords: Selective oxidation, 2.3- Dialdehydedextrin, 2.3- Dialdehydecellulose Sulfamic acid, 2.3- Dicarboxydextrin, 2.3- Dicarboxycellulose

1. Introduction

Functional derivatives of biopolymers are gaining increasing attention because they represent a sustainable, biocompatible, and biodegradable alternative to synthetic materials. Derivatives of cellulose, the most abundant naturally occurring biopolymer, are employed in a plethora of applications ranging from packaging materials and food additives to wound dressing (**Doelker, 1993**). Increasing attention has been dedicated to the selectively oxidized cellulose derivatives, such as 2,3-dialdehydecellulose (DAC, **Fig. 1**a) (**Kim, Kuga, Wada, Okano, & Kondo, 2000; Maekawa, 1991**), or 2,3-dicarboxycellulose (DCC, **Fig. 1**b) (**Kim & Kuga, 2001; Maekawa & Koshijima, 1984; Sirvio, Liimatainen, Visanko, & Niinimaki, 2014**), which offer number of unique characteristics in comparison with other cellulose derivatives.

The DAC is prepared by highly selective oxidation of cellulose hydroxyl groups at C2 and C3 to aldehydes by periodate (**Kim et al., 2000; Maekawa, 1991**). Raw insoluble DAC can be subsequently solubilized by hot water (**Kim, Wada, & Kuga, 2004**), which greatly expands its utilization in aqueous chemistry. Highly reactive aldehyde groups of DAC can be used to prepare microbeads and hollow

microspheres (**Lindh, Carlsson, Strpmme, & Mihranyan, 2014; Rocha, Ferraz, Mihranyan, Strpmme, & Lindh, 2018; Ruan, Strpmme, & Lindh, 2018; Yan et al., 2019**), antibacterial agents (**Ge, Zhang, Xu, Cao, & Kang, 2018**) or to crosslink hydrogels (**Kim et al., 2017; Munster, Capáková, Fišera, Kuřitka, & Vícha, 2019; Munster et al., 2018**). The presence of highly reactive aldehyde groups however also results in a rather complex structure of DAC in solution (**Maekawa, 1991; Spedding, 1960**) and contributes to its tendency to rapidly degrade unless kept under acidic conditions (**Munster et al., 2017**). Our recent NMR investigation of DAC structure in solution (**Munster et al., 2017**) revealed dominance of two prevailing structural motifs: the most abundant are two isomers of C3-O-C6 bonded intramolecular hemiacetal (**Fig. 1**c) with five-mem-bered "furanoid "cycle, which form about 70% of DAC. The second most abundant is C2'-O-C6 bonded intermolecular hemiacetal found in approx. 20% of DAC units, **Fig. 1**d. Note, that all aldehyde groups of DAC are hydrated in the aqueous solutions (**Munster et al., 2017; Spedding, 1960**).

Secondary oxidation of — CHO groups of DAC to — COOH by chlorite leads to the preparation of 2,3-dicarboxycellulose, DCC (**Maekawa & Koshijima, 1984; Sirvio et al., 2014**). On the contrary to DAC, the DCC with higher degree of oxidation (DO) has a well-defined structure and is well soluble in aqueous media without the need for solubilization (**Munster, Fojtů et al., 2019**). Partially oxidized DCC can be used for preparation of ultrafiltration membranes and chromatography columns (**Kim & Kuga, 2001; Visanko et al., 2014**), cellulose nanofibrils (**Tejado, Alam, Antal, Yang, & van de Ven, 2012**), highly-charged cellulose nanocrystals (**Yang, Alam, & van de Ven, 2013**), nanopaper (**Liimatainen, Visanko, Sirvio, Hormi, & Niinimaki, 2012**) or for water purification (**Suopajarvi, Liimatainen, Hormi, & Niinimaki, 2013**). Recently, we have used DCC with a high DO as a carrier for anticancer drug cisplatin with very good results (**Munster, Fojtů et al., 2019**).

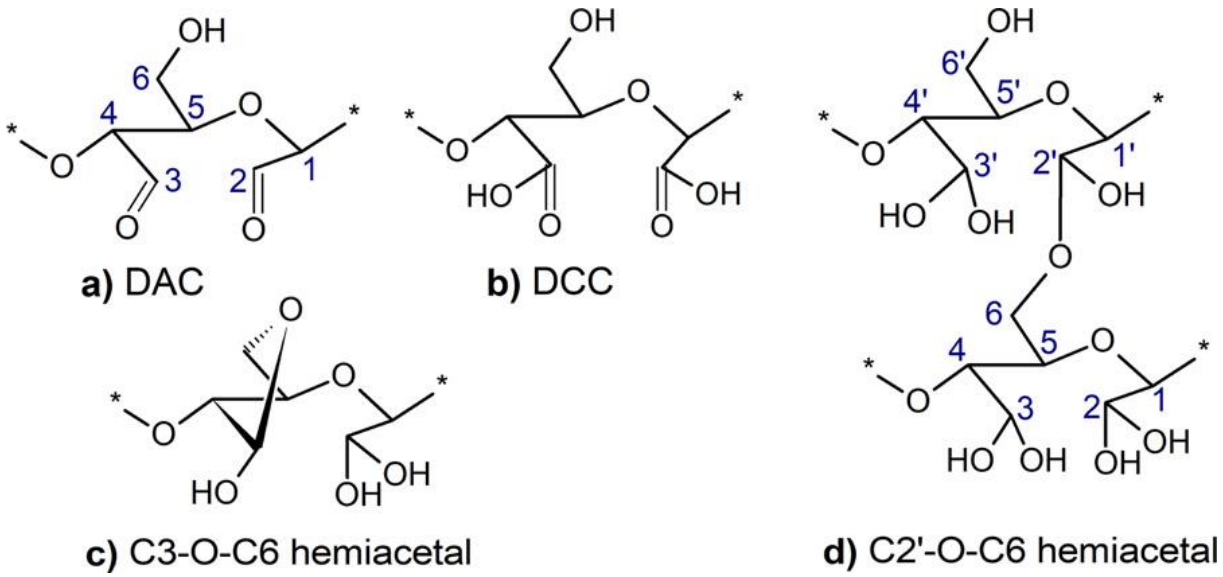

Fig. 1. Structure of a) 2,3-dialdehydecellulose, DAC, b) 2,3-dicarboxycellulose, DCC, c) C3-O-C6 bonded intramolecular hemiacetal, d) C2'-O-C6 bonded intermolecular hemiacetal.

Sulfamic acid (SAMAC) is usually added into the reaction mixture to enhance the effectivity of secondary oxidation of cellulose by scavenging of hypochlorite (**Sirvio et al., 2014**), which is generated in situ as a side product of secondary oxidation of DAC by chlorite, see Eq. (**1**).

$$R\text{–}CHO + HClO_2 \rightarrow RCOOH + HClO \quad (1)$$

Hypochlorite is a strong and non-selective oxidizing agent, which can react with remaining chlorite, Eq. (**2**), and potentially also with residual -OH groups of DAC. It is therefore generally deemed undesirable because it decreases the efficiency of the secondary oxidation and causes unwanted side-reactions.

$$HClO + 2ClO_2^- \rightarrow 2ClO_2 + Cl^- + OH^- \quad (2)$$

Hence, SAMAC is added to scavenge the hypochlorite and reduce the risk of side-reactions. One equivalent of SAMAC can react with two equivalents of hypochlorite, see Eqs. (**3**) and (**4**).

$$ClO^- + H_2NSO_3H \rightarrow ClNHSO_3H + H_2O \quad (3)$$

$$HClO + ClNHSO_3H \rightarrow Cl_2NSO_3H + H_2O \quad (4)$$

However, our recent study (**Munster, Fojtů et al., 2019**) revealed two previously unforeseen consequences of sulfamic acid addition to the reaction mixture. Firstly, the weight-average molecular weight of the product (M_w) was dependent on the molar amount of SAMAC - it decreased inversely with the increasing molar amount of SAMAC. Thus, Mw of DCC could be adjusted between ca. 20 and 100% of original material (DCC prepared without SAMAC), which allowed us to optimize the drug release rates. This increased the potency of drug-carrier conjugates against some cancer cell lines. Notably, the SAMAC-mediated decrease of Mw did not lead to increase of the polydispersity index (PDI) of the resulting material and appearance of very low-molecular weight fractions resulting in low yields of oxidized polysaccharide, which happens with other methods of molecular weight control (e.g. heating) (**Munster, Fojtů et al., 2019; Munster et al., 2017**). On the other hand, the decrease of M_w of DCC was achieved at the price of 10-15% decreased maximum DO - from more than 95% obtained in the SAMAC absence to 80-85%. This effect is not desirable as it somewhat reduces the maximum drug loading capacity of the DCC for cisplatin (about 5%) (**Munster, Fojtů et al., 2019**).

Based on observed results it was assumed that i) mechanism of SAMAC-catalyzed chain scission is likely more complex than simple acidic hydrolysis of cellulose chain ii) the control over the Mw of the product should be applicable also to other polysaccharides besides cellulose. To confirm these hypotheses, the mechanism of SAMAC-in-duced chain scission is elucidated in this work on an example of oxidized cellulose and modulation of Mw by SAMAC is investigated also for dextrin, branched polysaccharide obtained from starch or glycogen, composed from anhydroglucose units (AGU) bonded with 1-4' and 1-6' glycosidic bonds. Furthermore, the factors influencing the maximum achievable DO, the role of the molar ratio of reactants, their concentration, and the length of secondary oxidation are investigated for both cellulose and dextrin.

2. Materials and methods

2.1. Materials

SigmaCell type 20 (Sigma Aldrich Co.) was used as a source of cellulose and Dextrin from corn starch type I (Sigma Aldrich Co.) as a source of dextrin. Materials were characterized by FT-IR spectroscopy and X-ray diffraction, see Fig. S1 in Supporting Information. Cellulose has comparatively higher crystallinity than dextrin, which is reflected in different rates of primary oxidation, see below. Mw was estimated by GPC analysis to be 76kDa for cellulose and 51 kDa for dextrin (**Engel, Hein, & Spiess, 2012; Ferguson et al., 2018; Munster et al., 2017**). Sodium periodate ($NaIO_4$) and ethylene glycol (Penta, Czech Republic) were employed in the primary oxidation of polysaccharides. Acetic acid (>99.8%), sulfamic acid (99.3%), sodium chlorite (80%) (Sigma Aldrich Co.), sodium hydroxide (Lachner, Czech Republic) and sulphuric acid (96%) (Penta, Czech Republic) were used in secondary oxidation. All chemicals were of analytical grade and were used without further purification. Demineralized water was used throughout the experiment.

2.2. Preparation of 2,3-dicarboxypolysaccharide derivatives

Preparation of 2,3-dicarboxypolysaccharide derivatives was achieved via two-step sequential oxidation. In the first step, polysaccharide (cellulose or dextrin) was oxidized by using sodium periodate. In order to achieve the highest degree of oxidation, the molar ratio of reactants was set to 1:1.2 (polysaccharide : NaIO4). Typically, 16.5 g of $NaIO_4$ dissolved in 500 ml of water was used for oxidation of 10 g of source polysaccharide. The primary oxidation was performed at 30 °C in the absence of light to prevent spontaneous degradation of oxidation agent. Duration of oxidation step varied with the source of polysaccharide and was optimized by simple UV-VIS spectral analysis of periodate consumption (**Maekawa & Koshijima, 1984**). After there was no observable decrease in the intensity of the $NaIO_4$ absorption peak (222 nm), the primary oxidation was considered complete. Primary oxidation of cellulose and dextrin was found to be almost completed after 72 and 8 h, respectively. The difference is caused by variances in crystallinity (see Fig. S1) of selected polysaccharides (slower oxidation of cellulose crystallite cores) (**Calvini, Conio, Princi, Vicini, & Pedemonte, 2006**) and aqueous solubility of dextrin. The oxidation reaction was stopped by an excess of ethylene glycol and the resulting product was purified. Insoluble DAC was subjected to the repeated centrifugation and mechanical homogenization using WiseTis homo-genizer HD-15 (Witeg, Germany). Partially soluble 2,3-dialdehydedex-trin, DAD, was purified by 48 -h dialysis using dialysis tubing (Sigma Aldrich Co.) of 14 kDa molecular weight cut-off (MWCO). Both products of primary oxidation were then analysed in the terms of weight concentration of 2,3-dialdehydepolysaccharide in given volume of suspension/solution. The aldehyde content (DO from primary oxidation) of both prepared 2,3-dialdehydepolysaccharides was estimated via oxime reaction (**Veelaert, de Wit, Gotlieb, & Verhé, 1997**) to be 12.1 ± 0.6 (DO = 96.8 ± 4.8%). This was later verified by ^{1}H NMR spectra, where the intensity of the signals of non-oxidized anhy-droglucose units was found to be between 1-3% for all samples (relative to signals of corresponding 2,3-dicarboxypolysaccharides).

The secondary oxidation step involves oxidation of aldehydes by sodium chlorite in the presence of acetic acid. The reaction stoichiometry was set on the base of the molar ratio of reactants 1:4 (-CHO : $NaClO_2$), assuming 12.5mmol/g of — CHO groups which corresponds to fully oxidized dialdehydes. The concentration of $NaClO_2$ and acetic acid was set to 1 M and 0.5 M, respectively. The secondary oxidation starts by dropwise addition of the oxidation agent solution into the mixture containing 2,3-dialdehydepolysaccharide and acetic acid. The reaction was carried out at 30 °C in the absence of light for 7 h. After this period, the reaction was stopped by setting the pH to 10 by the addition of 10 M

NaOH. The solutions containing products of secondary oxidation (2,3-dicarboxycellulose, DCC and 2,3-dicarboxydextrin, DCD) were placed in dialysis tubing (MWCO =14kDa) and dialysed for 5 days for desalination and purification. The volume of samples was then reduced by rotary evaporator; pH was set to 7.4 by diluted NaOH; the samples were filtered and lyophilised. The resulting products prepared in the form of their sodium salt are designated as 2,3-dicarboxycellulose (DCC) and 2,3-dicarboxydextrine (DCD). Reaction yield was almost quantitative. The DO of the prepared 2,3-dicarboxypolysaccharides was estimated from ^{1}H NMR spectra. It represents the amount of cellulose units which hydroxyl groups were converted to carboxylic acids during the entire two-stage oxidation process. It is calculated as DO [%] = 100 IntAGU -IntHEMI, where IntAGU is the average intensity of the signals of — CH groups of residual anhydroglucose units, which were not oxidized during the primary oxidation, and IntHEMI is the average intensity of the signals of — CH groups of intermolecular hemiacetals which were not (fully) oxidized during secondary oxidation. Because no other species were detected in the spectra, the DO represents the total percentage of polysaccharide units converted to 2,3-dicarboxypolysaccharides.

2.3. Synthesis of DCC and DCD with different molecular weight

Modified secondary oxidation was employed to exemplify the role of SAMAC in molecular-weight control of DCC and DCD. Before the $NaClO_2$ addition, different amounts of 0.1mg/ml solution of SAMAC were added dropwise to 2,3-dialdehydepolysaccharide solution containing acetic acid. The molar ratio of SAMAC to — CHO was set to 0.125, 0.25, 0.5 and 1 mol of SAMAC to 1 mol of —CHO. In order to investigate the influence of oxidizing agent concentration and duration of secondary oxidation on M_w of resulting 2,3-dicarboxypolysacchar-ides, the concentration of $NaClO_2$ and duration of oxidation reaction was halved (i.e. to 0.5 M and to 3.5 h). The rest of the parameters and processes in DCC and DCD preparation remained the same.

2.4. Infrared analysis

FT-IR spectra were obtained by using Nicolet 6700 (Thermo Scientific, USA). Spectra were collected with ATR diamond crystal in the range of 4000 — 400 cm^{-1} with 64 scans and a resolution of 2 cm^{-1}.

2.5. X-ray diffraction analysis

XRD diffractograms of source polysaccharides noted in Supporting Information were performed on a Rigaku MiniFlex 600 diffractometer in the diffraction 2θ angle range 10-90°, $Co_{K\alpha}$ (X =1.789 Å) radiation source was used with Kβ line filter.

2.6. Elemental analysis

Prepared oxidized polysaccharides were analysed in terms of elemental composition by the energy-dispersive X-ray spectroscopy (EDS) using Oxford INCA Energy 200 system (Oxford Instruments, UK) equipped within scanning electron microscope Vega II/LMU (Tescan, Czech Republic) operated at 30 kV.

2.7. Molecular weight analysis

Gel permeation chromatography (GPC) was performed on prepared DCC and DCD samples using a Waters HPLC Breeze chromatographic system equipped with a Waters 2414 refractive index detector (temperature of drift tube 60 °C), Tosoh TSKgel GMPWXL column (300 x 7.8 mm x13 pm, column T =30 °C). A mixture of 0.1 M $NaNO_3$ and 0.05 M Na_2HPO_4 served as a mobile phase. Pullulan polysaccharide calibration kit SAC-10 (Agilent Technologies, Inc.) in a span of M_w 342-805 000 g/mol was used for calibration.

2.8. NMR analysis

All ^{1}H and ^{13}C NMR spectra were recorded using a Bruker Avance III HD 700 MHz NMR spectrometer equipped with a triple-resonance cryoprobe optimized for ^{13}C detection at 298 K in D_2O. Besides the 1D experiments, the ^{1}H-^{13}C heteronuclear single quantum correlation (HSQC, J_{H-C} =145 Hz) and 1H-13C heteronuclear multiple bond correlation (HMBC, nJH-C =10 Hz) experiments were performed (**Munster et al., 2017**).

2.9. Computational details

Structures were optimized by using B3LYP functional (**Lee, Yang, & Parr, 1988; Stephens, Devlin, Chabalowski, & Frisch, 1994**) and standard 6-31 G(d,p) basis set. The PCM solvent model was used to simulate aqueous environment (**Tomasi, Mennucci, & Cammi, 2005**). The D3 dispersion correction (**Grimme, 2006**) was included to improve the description of weak interactions. This setup provided good results in the past (**Babjaková et al., 2016; Čablová et al., 2017**).

3. Results and discussion

3.1. Mechanism of DCC chain scission in the presence of SAMAC

There are several possibilities for how SAMAC could cause chain scission. Firstly, the addition of SAMAC decreases the pH of the solution, which may trigger spontaneous acidic hydrolysis of 1-4' glycosidic bonds of DAC as is often exploited for cellulose (**Lelekakis, Wijaya, Martin, & Susa, 2014; Negahdar, Delidovich, & Palkovits, 2016**). To examine this possibility, series of secondary oxidations of DAC was performed using various amounts of SAMAC (from 1:0 to 1:1 —CHO: SAMAC molar ratio, see **Table 1** and Section **2.3** for experimental details). Results were compared with the analogical set of reactions in which SAMAC was replaced by sulphuric acid. The acidity of the solutions was kept in the same range of pH values (1.6-0.9, see **Table 1**).

Table 1 The molar ratio of —CHO groups of DAC and SAMAC, pH of the solution, weight-average molecular weight (Mw), degree of oxidation (DO) and polydispersity index (PDI) of DCC prepared using SAMAC and H_2SO_4, respectively.

	SAMAC					H_2SO_4			
Designation	DAC : SAMAC	pH	M_w [kDa]	*DO* [%]	*PDI*	pH	M_w [kDa]	*DO* [%]	*PDI*
DCC-0	1:0	2.3	74.8	96	1.95	2.3	74.8	97	1.77
DCC-0.125	1:0.125	1.6	71.4	95	1.95	1.6	75.1	97	1.75
DCC-0.25	1:0.25	1.4	21.1	84	1.65	1.4	74.9	97	1.74
DCC-0.5	1:0.5	1.1	20.2	86	1.65	1.1	75.7	97	1.78
DCC-1	1:1	0.9	29.8	94	1.65	0.9	75.6	97	1.75

Presumably, if the DCC chain scission is indeed caused purely by acidic hydrolysis of 1-4' glycosidic bonds, both series should lead to similar results. Reactions were terminated after 7 h, and products were dialysed and lyophilised. M_w of all samples was estimated by GPC and degree of oxidation was determined from ^{1}H NMR spectra. To rule-out the possible buffering effect of acetic acid in the solution, the same reactions were repeated in its absence. The reaction performed without acetic acid however led to the destruction of DAC macromolecules (products of brown colour with M_w between 3-9 kDa). The presence of acetic acid in the reaction mixture is thus clearly essential for successful secondary oxidation. Most likely, acetic acid buffers the solution and sustains the acidic pH even after addition of basic $NaClO_2$ salt, which stabilizes the dialdehydes and prevents their degradation in basic pH (**Munster et al., 2017**).

Considerable differences in both M_w and DO were observed between the SAMAC and H_2SO_4 series. The addition of SAMAC causes an expected decrease of Mw already for DCC-0.125 sample (— CHO : SAMAC ratio of 1:0.125) and reaches maximum for DCC-0.5. Note, that Mw of DCC-1 prepared using 1:1 ratio of —CHO : SAMAC is higher than in case of DCC-0.5. The DO of DCC follows the same V-shaped trend. The DO established from 1H NMR spectra ranges between 96% (DCC-0) and 84% (DCC-0.25). Reasons behind DO modulation are discussed in the following Section 3.2, here we focus exlusively on the modulation of M_w.

In contrast to the SAMAC series, the addition of H_2SO_4 has no observable effect on the Mw of DCC. In other words, no sign of acidic hydrolysis of DCC chains was observed in given range of pH. The DCC chain scission is thus more effective for SAMAC than for sulphuric acid solution. This is rather surprising because acidic hydrolysis of cellulose is known to strongly depend on the strength (pKa) of the acid (**Rinaldi, Meine, vom Stein, Palkovits, & Schuth, 2010**). Another difference can be found in the comparison of polydispersity indexes (PDI), see **Table 1**. The PDI of the products prepared by using H_2SO_4 remain roughly the same (1.7 ± 0.1). For comparison, the PDI of samples prepared by using SAMAC is steadily decreasing from 1.95 to 1.65. The mechanism of SAMAC-induced DCC chain scission is thus not based on a simple mechanism of acidic hydrolysis.

To answer the question of what causes the high effectivity of SAMAC in DCC chain scission, we have considered known differences between chemistry of SAMAC and H_2SO_4. One of the key differences is the effectivity of sulfonation reactions. Sulphuric acid is a much weaker sulfonating agent than SAMAC (**Benson & Spillane, 1980; Wagenknecht, Nehls, & Philipp, 1993**). Moreover, SAMAC is also known to react readily with both aldehydes and ketones at normal temperature (**Chen, Qin, & Jin, 2007; Luo, Kang, Nie, & Yang, 2009; Sarkate, Sangshetti, Dharbale, Sarkate, & Shinde, 2015**). Therefore, SAMAC may be able to directly sulfonate aldehydic/gem-diol groups (hydrated aldehydes) at C2 and C3 of DAC even at mild conditions. On the other hand, sulfo-nation of hydroxyl groups of DAC/DCC by SAMAC is unlikely, because high temperature, organic solvent, and urea as a catalyst are necessary for sulfonation of —OH groups of cellulose (**Wagenknecht et al., 1993**).

Let us now consider possible consequences of sulfonation of aldehyde groups at C2 and C3 of DAC. Sulfonation of aldehyde group(s) will bring highly acidic -SO_3H group to the close vicinity of the oxygen atom of 1-4' glycosidic bond. It can thus effectively protonate O4', which may trigger the acidic hydrolysis. The -SO_3— group is then eliminated from aldehyde groups during their oxidation to the carboxylic acid by ClO_2 — (no signals of sulfonated C2 or C3 were detected in NMR spectra of DCC, see below). The suggested mechanism of this “sulfonation-induced scission” is shown in **Scheme 1**. To a certain extent, it resembles the action of acidic solid-state catalysts used in depolymerisation of cellulose (**Shrotri, Kobayashi, & Fukuoka, 2018**).

To prove the suggested mechanism, the DAC was dissolved in the mixture containing acetic acid and 1 molar equivalent of SAMAC (relative to — CHO groups of DAC), which was stirred in the absence of light for 7 h. This setup mimics conditions used for secondary oxidation of DAC, albeit in the absence of an oxidizing agent. Obtained sample, DAC-S (abbreviation from DAC-SAMAC), was subsequently dialyzed against demineralized water for 5 days in order to remove all traces of unbound SAMAC and lyophilised. The amount of sulphur in resulting material was then determined by EDS analysis. Results were compared with DCC-1 sample prepared using standard oxidation scheme with the same amount of SAMAC as DAC-S. Presumably, if the — CHO groups of DAC are sulfonated according to Scheme 1, the content of sulphur should be much higher in the DAC-S than in DCC-1. Indeed, the measured content of sulphur in DAC-S was 4.2 ± 0.8 at%, while in case of DCC-1 it was 20-times less with 0.2 ± 0.04 at%. Assuming that aldehyde carbons C2 and C3 form about 15 at% of each hydrated DAC unit (consisting of six carbon and seven oxygen atoms) and about one half of them is involved in variety of hemiacetal bonds (**Munster et al., 2017**), the significant portion of remaining hydrated aldehyde (gem-diol) groups is sulfonated. Lower content of sulphur in DCC-1 sample agrees with presumed elimination of -SO_3H groups from DAC during secondary oxidation. These findings support suggested reaction mechanism, **Scheme 1**.

At this point, it is necessary to note that there are two possible pathways of SAMAC addition to hydrated aldehyde groups found in DAC solutions (gem-diols) (**Munster et al., 2017**). The -SO_3H may either attach directly to aldehyde carbon (assuming simultaneous elimination of water from gem-diol) (**Liimatainen, Visanko, Sirvio, Hormi, & Niinimaki, 2013**) or via one of the hydroxyl groups of gem-diol (**Benson & Spillane, 1980**), forming essentially a DAC ester of sulphuric acid. Although the latter mechanism seems to be more likely in an aqueous environment, neither pathway could be ruled out immediately. Therefore, the FT-IR spectra of DCC-0 (0 at% of sulphur, prepared without SAMAC) and DCC-1 (with 0.2 ± 0.04 at.% of S) were measured, subtracted and analysed, see **Fig. 2**. Observed bands were assigned to vibrations of O=S=O and S—O groups (621 and 1117 cm^{-1}). No bands corresponding to S—C bonds vibration modes were detected in the spectra, which supports the predominant formation of DAC-sulphuric acid ester structure. The analysis was performed using DCC FT-IR spectra because direct comparison of DAC and DAC-S was not feasible due to spectral changes (hemiacetal breaking) caused by dissolving the latter in acidic SAMAC solution.

Moreover, DFT calculations were used to simulate the structures of DAC sulfonated at C2 (C2-SO_3H) and DAC sulphuric acid ester (C2-O-SO_3H) to further investigate the mode of binding of -SO_3H and to determine the distances between the -SO_3H group and the oxygen atom of 1-4' glycosidic bond. The C2 of DAC was selected as the most likely target for sulfonation reaction because C3 of DAC is in solution mostly bound in C3-O-C6 hemiacetal (**Fig. 1**c). Besides, the C2 is known to be a preferred target for sulfonation reactions in cellulose (after C6) (**Zhang, Brendler, Geissler, & Fischer, 2011**). Initially, the model structure of DAC composed from twelve monomeric units in their most abundant form of intramolecular C3-O-C6 hemiacetal was optimized at B3LYP/6-31G(d,p) level of theory, which provided a good results in the past (**Babjaková et al., 2016; Čablová et al., 2017**). In the following step, the central unit of each structure was modified by C2-SO_3H and C2-O-SO_3H groups, respectively. Structures were reoptimized at the same level of theory and their central parts are shown in **Fig. 3**.

The calculated distance between the proton of -SO_3H group and the oxygen atom of 1-4' glycosidic bond for C2-O-SO_3H (ester structure) is only 1.61 A, see **Fig. 3**. This is much shorter than the sum of vdW radii of H and O. One may expect a protonation equilibrium between -SO_3H and O4' to form rather easily. On the other hand, the distance between O4' and -SO3H in C2-SO_3H structure is 2.25 A, which is likely caused by the formation of second, 1.84 A long hydrogen bond between -SO_3H group and O6' from nearby C3-O-C6 intermolecular hemiacetal ring, **Fig. 3**. The C2-SO3H structure thus seems less

suitable for protonation of O4', but may be partly responsible for the absence of C3-O-C6 intramolecular hemiacetal rings in the final product despite their high abundance in DAC.

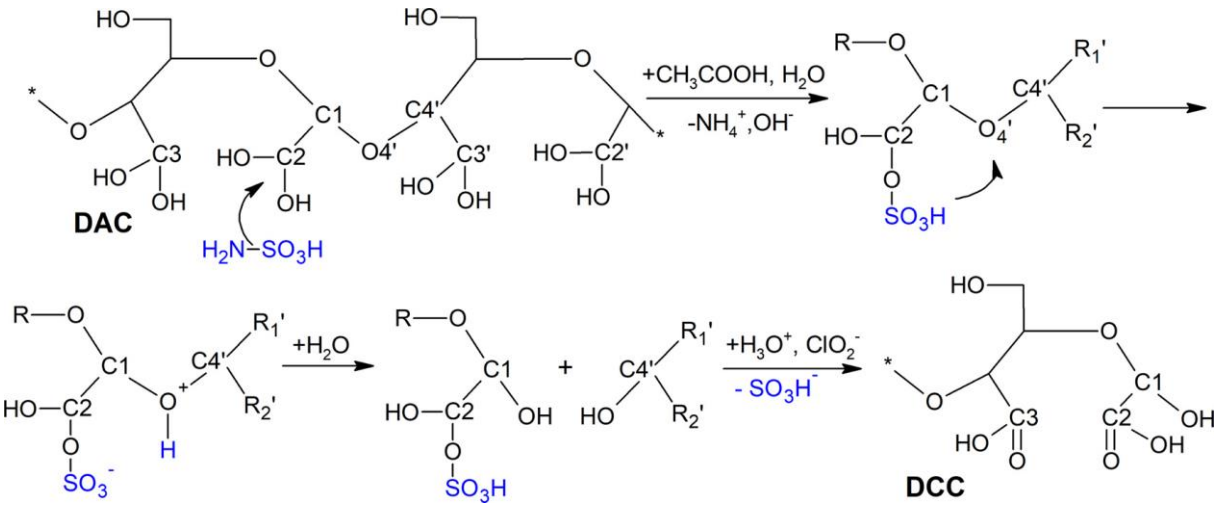

Scheme 1. The mechanism of sulfonation of — CHO group at C2 of 2,3-dialdehydecellulose (DAC) and subsequent acidic hydrolysis of 1-4' glycosidic followed by elimination of -SO3H- group during the secondary oxidation of aldehydes to 2,3-dicarboxycellulose (DCC).

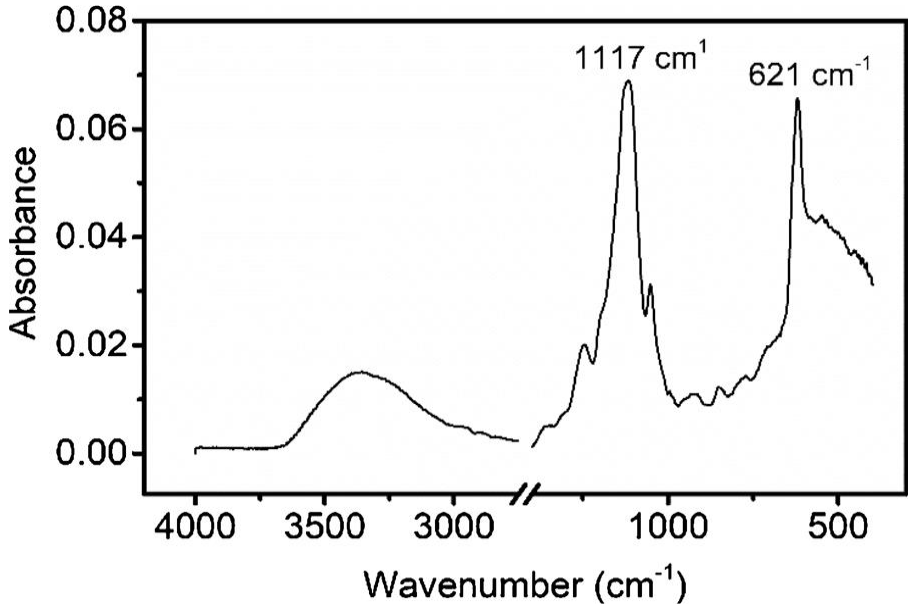

Fig. 2. Difference of FT-IR spectra of DCC-1 (2,3-dicarboxycellulose prepared by using 1 molar equivalent of sulfamic acid) and DCC-0 (prepared in the absence of sulfamic acid), showing the S—O (1117 cm^{-1}) and O=S=O (621 cm^{-1}) vibration modes.

Based on observed data and supporting calculations, it is assumed that addition of SAMAC during secondary oxidation causes sulfonation of aldehyde/gem-diols groups of DAC, with the -SO_3H groups bound most likely via oxygen atom of gem-diol group (see **Scheme 1**). The -SO_3H groups are then in an ideal position to protonate the oxygen atom of 1-4' glycosidic bonds, which may trigger acidic

hydrolysis, causing DAC chain scission. The -SO_3H groups are subsequently eliminated from the material during oxidation of DAC to DCC.

3.2. The degree of oxidation of DCC in the presence of SAMAC

As mentioned above, the addition of SAMAC influences also the DO. Let us first recall the trends in DO from **Table 1**. DO of DCC does not decrease linearly with the increasing amount of SAMAC as one may expect, but the minimum (84%) is reached for DCC-0.25, with DCC-0.5 only marginally better (86%). No such dependence is observed for materials prepared in the presence of sulphuric acid (DO 97%). Observed minima are thus likely related to another feature of SAMAC - the hypochlorite scavenging, which is not possible with H_2SO_4. To investigate, the ^{1}H, ^{13}C and ^{1}H-^{13}C HSQC and HMBC correlation spectra of DCC-0 (DO = 96%) and DCC-0.25 (DO = 84%) were recorded and analyzed, see **Table 2** and **Fig. 4**.

Beside DCC itself, two minor species were detected in both spectra. The first set of signals was assigned to the residual anhydroglucose units of cellulose (AGU), which were not oxidized during primary oxidation. The second set was identified as former C6-O-C2' hemiacetals (**Fig. 1**d), partially oxidized in positions 2, 3 and 3' during the secondary oxidation, see **Fig. 4**. This molecule was unequivocally identified based on distinct correlation signals between C6/H6 and C2'/H2' (**Munster, Fojtů et al., 2019; Munster et al., 2017**). Its signals are marked with asterisks in **Fig. 4** and signal assignment is given in **Table 2**.

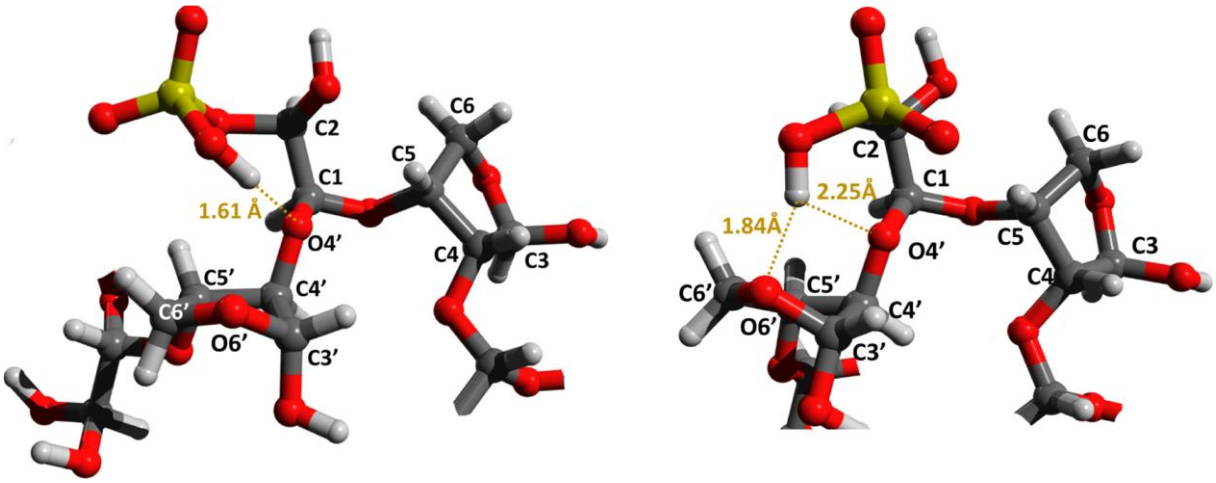

Fig. 3. DFT optimized structures of DAC (2,3-dialdehydecellulose) sulphuric acid ester (left) and sulfonate (right). The distance between proton of -SO3H group and closest oxygen atom(s) is highlighted. More distant DAC residues are omitted for clarity.

Table 2 The 2H and 13C NMR chemical shifts assignment for DCC and partially oxidized DCC C2-O-C6 hemiacetal.

		1	2	3	4	5	6 (6^a/6^b)
DCC	^{1}H	4.70	–	–	3.99	4.03	3.68
	^{13}C	101.0	173.7	176.1	79.9	77.7	60.8
DCC C2'–O–C6	^{1}H	4.73	–	–	3.99	4.36	4.07/3.42
	^{13}C	101.6	173.8	175.2	77.8	67.8	57.3
	^{1}H'	4.62	4.78	–	4.04	4.18	3.61/-
	^{13}C'	96.8	88.0	176.0	80.0	78.4	60.5

The signal intensity of residual AGUs is approximately 1% relative to signals of DCC in both cases, which illustrates the high effectivity and good reproducibility of primary oxidation. On the other side, the signals of C6-O-C2' hemiacetal are much stronger in DCC-0.25 (15% intensity relative to DCC) than in DCC-0 (3%). For comparison, the amount of C6-O-C2' hemiacetals in neat DAC solution was estimated to ca. 20% (**Munster et al., 2017**). The presence of SAMAC in the reaction mixture (above 0.25:1 molar ratio) apparently "protects" inermolecular hemi-acetals from secondary oxidation and thus reduces maximum achievable DO.

A possible explanation can be found in differences between mechanisms of oxidation of aldehydes by chlorite and hypochlorite, respectively, in combination with hypochlorite scavenging ability of SAMAC. The mechanism of oxidation of the aldehyde group by chlorite is shown in **Scheme 2**a (**Sirvio et al., 2014**). The reaction starts with the addition of O-Cl = O — to the aldehyde carbon in an acidic environment with the simultaneous breaking of the C=O double bond (**Sirvio et al., 2014**). However, this mode of action could not be directly employed for hemiacetals. In such a case, the hemiacetal bond needs to be first hydrolyzed and an aldehyde group re-formed. Because intermolecular hemiacetals are stabilized by inductive effects of large polysaccharide residues, not mentioning possible steric hindrance, their hydrolysis will likely become the rate-determining step. The efficiency of oxidation of these groups by chlorite will thus be significantly reduced.

On the other hand, hypochlorite can oxidize hemiacetal directly to the ester of carboxylic acid, because the reaction runs on the available hydroxyl oxygen atom, **Scheme 2**b. Breaking of hemiacetal bond is thus not required. The resulting DCC C6-O-C2' ester could hydrolyze easily in the acidic environment of the reaction mixture, which results in the formation of DCC, **Scheme 2**b.

The indices supporting suggested mechanism can be deduced from the observed trend of DO in different concentrations of SAMAC. It seems to be a result of an interplay of two factors: i) the hypochlorite scavenging which protects intermolecular hemiacetals from oxidation according to **Scheme 2**b; ii) increased rate of chlorite oxidation of hemiacetals (**Scheme 2**a) due to more acidic environment (increasing concentration of SAMAC). In theory, each SAMAC molecule is capable of reaction with two molecules of hypochlorite, see Eq. (**3**) and (**4**). Hence, the SAMAC : — CHO ratio of 0.5 : 1 ensures complete scavenging of generated hypochlorite. In the real system, part of the hypochlorite is however bound to react with other targets, particularly with the highly abundant ClO_2 —, see Eq. (**2**). As a result, already the 0.25 molar equivalent of SAMAC seems to be capable of scavenging the remaining hypochlorite and thus protecting C6-O-C2' hemiacetals. Lower pH of DCC-0.5 and particularly DCC-1 solution causes faster hydrolysis in comparison with DCC-0.25, which leads to subsequent oxidation of hemiacetals according to **Scheme 2** and to the increase of DO.

We attempted to prove the importance of hypochlorite for the oxidation of hemiacetals (Scheme 2b) by performing tertiary oxidation of DCC-0.25 with 15% of DCC C2'-O-C6 hemiacetals using solely hypochlorite. Up to two equivalents of hypochlorite (relative to the amount of residual DCC C2'-O-C6 hemiacetal) were added to the mixture in the presence of acetic acid and stirred for 7 h in the dark to mimic the conditions of secondary oxidation. However, these attempts did not bring the desired results. Hypochlorite caused a partial degradation of DCC and resulting complex NMR spectra of the product prohibited analysis of residual hemiacetal content (signal overlap). Most likely, we were unable to replicate a relatively slow generation of hypochlorite in situ. The proposed mechanism thus cannot be unequivocally proven at the moment.

The role of SAMAC for the M_w and DO of the product was investigated for cellulose derivatives. However, will these results be valid also for other polysaccharides? Is the fine-tunning of Mw possible, while keeping the DO above 90% at the same time? To find out, the optimization of secondary oxidation of both cellulose and dextrin was performed to obtain products with variable M_w and with highest possible DO.

3.3. Optimization of secondary oxidation of cellulose and dextrin

Cellulose and dextrin were oxidized to DCC and DCD, respectively, by the two-stage oxidation process, see Sections **2.2** and **2.3** for more details. While the primary oxidation of cellulose is well-documented (**Kim et al., 2000; Munster, Fojtů et al., 2019; Munster et al., 2017**), data about primary oxidation of dextrin lacks. Therefore, the kinetics of primary oxidation of both materials was briefly investigated by observing the consumption of periodate over time (**Maekawa & Koshijima, 1984**). While DAC with DO > 95% is obtained after 72 h of primary oxidation, for DAD it is only 8 h. This difference is due to better solubility and lower crystallinity of dextrin compared to cellulose (see Fig. S1) (**Calvini et al., 2006**).

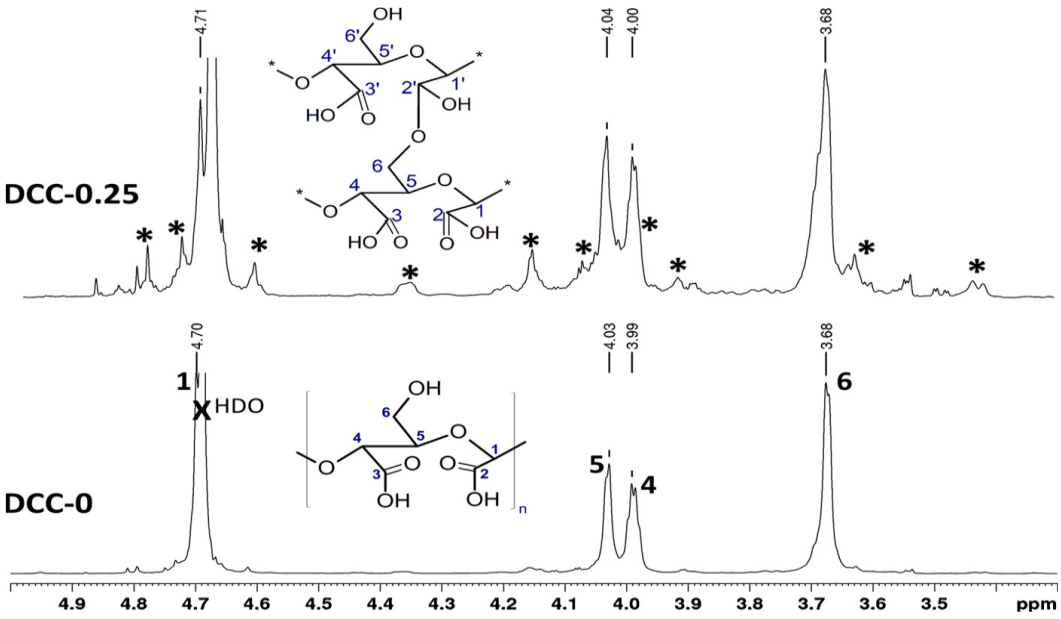

Fig. 4. ^{1}H spectra of DCC-0 (2,3-dicarboxycellulose prepared without sulfamic acid) with the structure of DCC (bottom) and DCC-0.25 (2,3-dicarboxycellulose prepared by using 0.2 molar equivalent of sulfamic acid) with the structure of partially oxidized C6-O-C2' hemiacetal (top). Signals of hemiacetal are marked with asterisks, see **Table 2** for assignment.

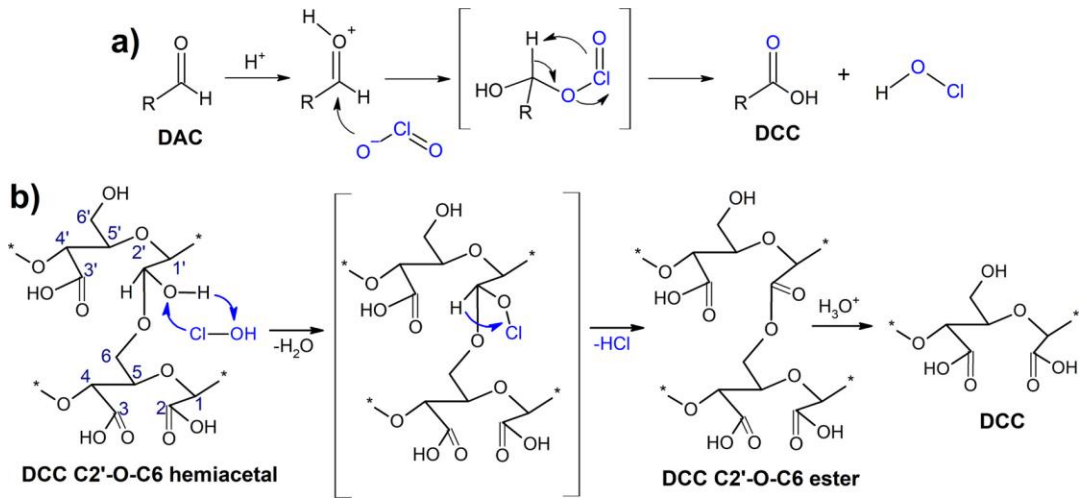

Scheme 2. a) the mechanism of chlorite oxidation of aldehyde, b) the mechanism of hypochlorite oxidation of partially oxidized C2'-O-C6 hemiacetal.

Resulting 2,3-dialdehydepolysaccharides were subsequently oxidized by chlorite. Secondary oxidation of both materials was performed using different conditions: i) various molar equivalents of SAMAC (up to 1:1 SAMAC : —CHO ratio, see **Table 1**), ii) different concentrations of the reactants (0.5 and 1 mol/L of chlorite) and iii) oxidation times (3.5 and 7 h). The DO and M_w of the products were investigated by using NMR and GPC analysis and results are given in Supporting Information, Tables S1 and S2 and Figs. S2-S8. Different conditions of secondary oxidation are emphasized by upper and lower index in sample notation. For instance, DCC prepared without SAMAC and by using shorter oxidation time is noted as DCC-$0^{3.5}$, while the same sample prepared by using 0.5 mol/L concentration of chlorite is noted as DCC-$0_{0.5}$.

The M_w of DCC, DCC$^{3.5}$, and DCC$_{0.5}$ as a function of the SAMAC molar ratio is given in **Fig. 5**a. Addition of SAMAC causes a decrease of Mw of DCC from ~70kDa to ~18kDa, i.e. to approximately one-quarter of the original value. This agrees well with previous observations (**Munster, Fojtů et al., 2019**). Increase of M_w observable in all DCC-1 samples can be attributed to increased effectivity of chlorite oxidation in lower pH, which partially prohibits the sulfonation and thus also the chain scission.

Interestingly, shortening the secondary oxidation to 3.5 h has minimal effect on the M_w of the product, although it slightly decreases the maximum DO of some samples, see **Fig. 5** and the corresponding discussion below it. Lower concentration of reactants, on the other hand, influences the M_w of DCC considerably and leads to the preparation of DCC0 5 samples with Mw 30-70 kDa, see **Fig. 5**a and Table S1. The largest difference in M_w caused by different concentration of reactants is observed for DCC-0.25 and DCC-0.250.5, respectively. Lower concentrations of chlorite salt leads to 2.5-times higher M_w in the latter (21 kDa vs. 52 kDa).

The degree of oxidation of DCC follows the trends described in the previous section, i.e. minimum is found in all DCC-0.25 samples, see Table S1. While the decrease of the duration of oxidation has a relatively small effect to DO (see Table S1), lower concentration of reactants allows preparing of DCC with DO above 90% in all cases. Most likely, SAMAC is less effective in scavenging of hypochlorite at lower concentrations, and the hemiacetals are thus oxidized more efficiently according to **Scheme 2**b.

Dependences of M_w of DCD samples on SAMAC molar ratio are given in **Fig. 5**b. Observed trends in of M_w of DCD resemble those of DCC. The M_w of DCD prepared using standard conditions, i.e. 1 mol/L

concentration of chlorite and 7 -h oxidation duration, decreases from 43 kDa to 15 kDa (35%). However, secondary oxidation of DCD at these conditions led to partial degradation of the product, hence lower Mw of DCD-0. This is best observable in NMR spectra of DCD series, see Fig. S5. Note that NMR spectra were improving with the increasing amount of SAMAC (lower pH).

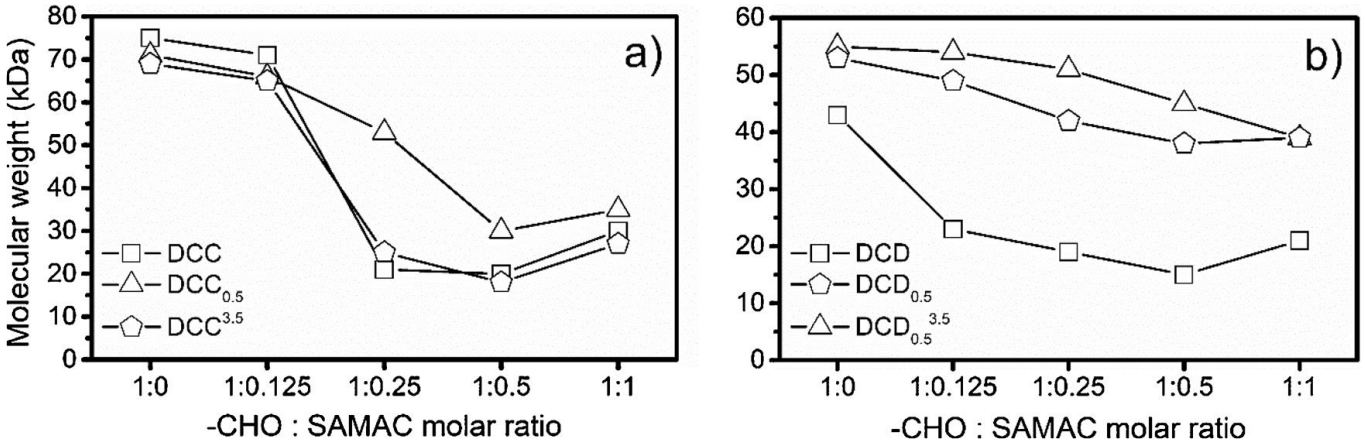

Fig. 5. Dependence of Mw of a) 2,3-dicarboxycellulose, DCC, b) 2,3-dicarboxydextrin DCD on the molar ratio of sulfamic acid (SAMAC) in the reaction with respect to different reaction conditions (concentration, time).

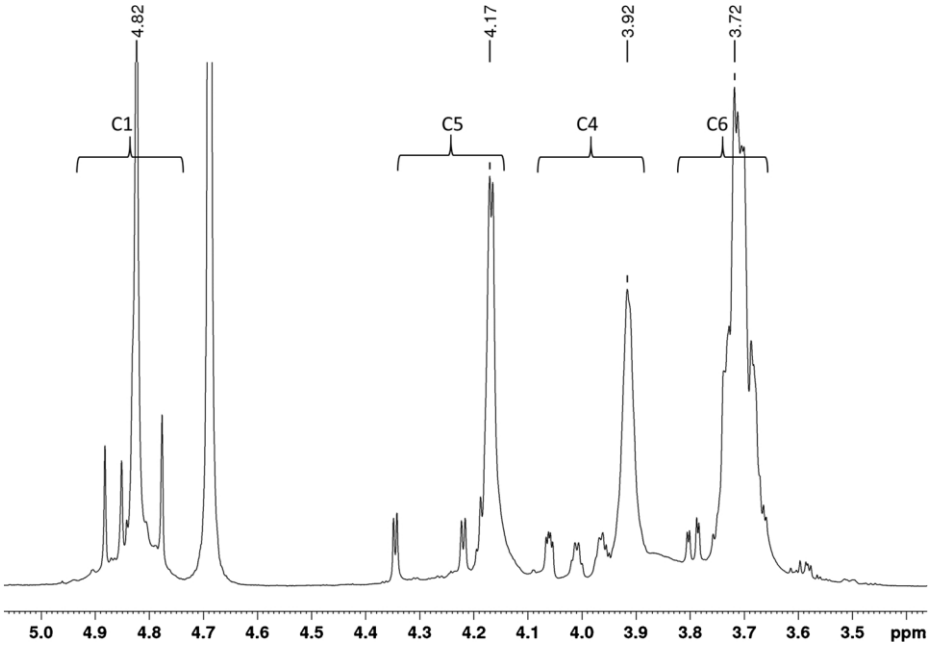

Fig. 6. ^{1}H NMR spectra of DCD-0, 2,3-dicarboxydextrin prepared in the absence of sulfamic acid, minor signals are caused by of 1-6' branching of dextrin chain (**Petersen et al., 2015**).

On the other hand, DCD05 materials are of a good purity and of Mw between 53 and 38 kDa (70%). Hence, to avoid degradation, the role of oxidation time was studied for more diluted solutions of 0.5 mol/L concentration of chlorite (DCD0.5 series). The resulting material is designated as DCD0.53.5. Decrease of duration of secondary oxidation did not influence minimal achieved Mw of DCD, which is the same as for DCD05 (38 kDa). However, the decrease is continuous and more linear than in DCD05

series, and the lowest M_w is achieved for SAMAC : -CHO ratio of 1:1, not 0.5:1 as before, see **Fig. 5**b. The smaller influence of SAMAC to Mw of DCD (in comparison with DCC) may be related to 1-6' branching of dextrin, which is from principle less susceptible to SAMAC-induced chain scission.

To determine the DO of DCD, its ^{1}H NMR spectra were measured and assigned. ^{1}H NMR spectrum of DCD-00.5 (prepared without SAMAC) is shown in **Fig. 6**, and the assignment is given in Table S3 in Supporting Information. For the other NMR ^{1}H spectra see Figs. S5, S6, and S7 in Supporting Information. Minor signals in the spectra were identified based on multiplicity edited ^{1}H-^{13}C HSQC spectra (Fig. S8) as a 1-6' branching of DCD units (**Petersen, Motawie, M0ller, Hindsgaul, & Meier, 2015**). These units form about 10% of DCD (relative to the signal intensity of major DCD signals).

^{1}H NMR spectra of DCD05 and DCD0535 revealed DOs between 94-97%, with only small amounts of C6-O-C2' hemiacetals (1-3%). This is likely another result of 1-6' branching of dextrin, which renders the formation of C6-O-C2' hemiacetals in 2,3-dialdehydedextrin (DAD) solutions less favorable than in case of DCC. Amount of non-oxidized AGUs was between 2-3% in all cases, which indicates high effectivity of primary oxidation.

4. Conclusions

Sulfamic acid (SAMAC) can be used to control the weight-average molecular weight (M_w) of various 2,3-dicarboxypolysaccharides containing 1-4' glycosidic bonds, which was demonstrated for oxidized cellulose and dextrin. Initial hypothesis suggesting a rather complex mechanism of action was confirmed, because scission of 2,3-dicarbox-ypolysaccharide chains is not caused by simple acidic hydrolysis. Instead, it is initiated by sulfonation of hydrated aldehyde groups (gem-diols) of corresponding 2,3-dialdehydepolysaccharides. The -SO_3H groups bound to gem-diols via available hydroxyl groups can effectively protonate the oxygen atoms of 1-4' glycosidic bond and thus trigger the chain scission. The -SO_3H- groups are subsequently eliminated during oxidation of aldehydes to carboxylic acids. The suggested reaction mechanism is supported by a comparative study with sulfuric acid (not capable of sulfonation), NMR, GPC, EDS, FT-IR analyses, and DFT calculations.

Additional investigation revealed that the Mw of 2,3-dicarbox-ycellulose (DCC), which contains exclusively 1-4' glycosidic bonds, can be modulated in between 25-100% of DCC prepared without SAMAC. Finer control over the Mw can be achieved by reducing the concentration of chlorite. The control over the Mw of 2,3-dicarboxydextrin (DCD) is also possible, but the effect of SAMAC is less pronounced, as the Mw of DCD can be reduced only by 30%, probably due to presence of 1-6' glycosidic bonds in dextrin structure. Further decrease of M_w may however be possible by increasing the SAMAC :-CHO of dextrin molar ratio, while simultaneously shortening the duration of the oxidation and keeping the concentration of chlorite <0.5 mol/L in order to avoid degradation.

Slightly lower maximum achievable degree of oxidation (DO) in the presence of SAMAC was traced to the persistence of intermolecular hemiacetal bonds. The reason being that SAMAC is, at least in larger concentrations, capable of scavenging the in situ generated hypochlorite before it can oxidize hemiacetals to the esters of carboxylic acids. Suggested mechanism is supported by indirect evidence (dependence of DO on molar amount and concertation of SAMAC), because attempts to perform tertiary oxidation of hemiacetals using hypochlorite resulted in the mixture of products and very complex NMR spectra. Subsequent optimization of reaction conditions revealed that to obtain DCC with adjustable M_w and DO above 90%, one should use longer secondary oxidation in combination with a lower concentration of reactants. No special treatment is required for dextrin, where only trace amounts of hemiacetals persist after secondary oxidation, probably due to 1-6' branching.

To summarize, the use of SAMAC allows to effectively control the Mw of the 2,3-dicarboxypolysaccharides without risk of uncontrolled degradation of the material and appearance of very low-molecular weight fraction, which is associated with other methods of molecular weight reduction like solubilization or heating (**Munster et al., 2017**). Resulting product can be obtained in quantitative yields, has a high purity and molecular weight distribution (expressed by polydispersity index, PDI) comparable or better than that of original material. To the best of our knowledge, presented mechanism of sulfonation-catalyzed chain scission is unique and might find applications in the preparation of drug delivery systems with molecular weight-controlled drug release rates or it may inspire the development of new synthetic approaches in the future.

References

Babjaková, E., Branná, P., Kuczynska, M., Rouchal, M., Prucková, Z., Dastychová, L., et al. (2016). An adamantane-based disubstituted binding motif with picomolar dissociation constants for cucurbit[n]urils in water and related quaternary assemblies. RSC Advances, 6(107), 105146-105153. https://doi.org/10.1039/C6RA23524G.

Benson, G. A., & Spillane, W. J. (1980). Sulfamic acid and its N-substituted derivatives. Chemical Reviews, 80(2), 151-186. https://doi.org/10.1021/cr60324a002.

Čablová, A., Rouchal, M., Hanulíková, B., Vícha, J., Dastychová, L., Prucková, Z., et al. (2017). Gas-phase fragmentation of 1-adamantylbisimidazolium salts and their complexes with cucurbit[7]uril studied using selectively 2 H-labeled guest molecules. Rapid Communications in Mass Spectrometry, 31(18), 1510-1518. https://doi.org/10. 1002/rcm.7919.

Calvini, P., Conio, G., Princi, E., Vicini, S., & Pedemonte, E. (2006). Viscometric determination of dialdehyde content in periodate oxycellulose Part II. Topochemistry of oxidation. Cellulose, 13(5), 571-579. https://doi.org/10.1007/s10570-005-9035-y.

Chen, W.-Y., Qin, S.-D., & Jin, J.-R. (2007). Efficient biginelli reaction catalyzed by sulfamic acid or silica sulfuric acid under solvent-free conditions. Synthetic Communications, 37(1), 47-52. https://doi.org/10.1080/00397910600977632.

Doelker, E. (1993). Cellulose derivatives. In R. S. Langer, & N. A. Peppas (Vol. Eds.), Biopolymers I: VoL 107, (pp. 199-265). . https://doi.org/10.1007/BFb0027554.

Engel, P., Hein, L., & Spiess, A. C. (2012). Derivatization-free gel permeation chromatography elucidates enzymatic cellulose hydrolysis. Biotechnology for Biofuels, 5(1), 77. https://doi.org/10.1186/1754-6834-5-77.

Ferguson, E. L., Naseer, S., Powell, L. C., Hardwicke, J., Young, F. I., Zhu, B., et al. (2018). Controlled release of dextrin-conjugated growth factors to support growth and differentiation of neural stem cells. Stem Cell Research, 33, 69-78. https://doi.org/10. 1016/j.scr.2018.10.008.

Ge, H., Zhang, L., Xu, M., Cao, J., & Kang, C. (2018). Preparation of dialdehyde cellulose and its antibacterial activity. In H. Liu, C. Song, & A. Ram (Vol. Eds.), Advances in applied biotechnology: Vol. 444, (pp. 545-553). . https://doi.org/10.1007/978-981-10-4801-2_56.

Grimme, S. (2006). Semiempirical GGA-type density functional constructed with a long-range dispersion correction. Journal of Computational Chemistry, 27(15), 1787-1799. https://doi.org/10.1002/jcc.20495.

Kim, U.-J., & Kuga, S. (2001). Ion-exchange chromatography by dicarboxyl cellulose gel. Journal of Chromatography A, 919(1), 29-37. https://doi.org/10.1016/S0021-9673(01)00800-7.

Kim, U.-J., Kuga, S., Wada, M., Okano, T., & Kondo, T. (2000). Periodate oxidation of crystalline cellulose. Biomacromolecules, 1(3), 488-492. https://doi.org/10.1021/ bm0000337.

Kim, U.-J., Lee, Y. R., Kang, T. H., Choi, J. W., Kimura, S., & Wada, M. (2017). Protein adsorption of dialdehyde cellulose-crosslinked chitosan with high amino group contents. Carbohydrate Polymers, 163, 34-42. https://doi.org/10.1016/j.carbpol. 2017.01.052.

Kim, U.-J., Wada, M., & Kuga, S. (2004). Solubilization of dialdehyde cellulose by hot water. Carbohydrate Polymers, 56(1), 7-10. https://doi.org/10.1016/j.carbpol.2003. 10.013.

Lee, Ch., Yang, W., & Parr, R. G. (1988). Development of the Colle-Salvetti correlation-energy formula into a functional of the electron density. Physical Review B, 37(2), 785-789. https://doi.org/10.1103/PhysRevB.37.785.

Lelekakis, N., Wijaya, J., Martin, D., & Susa, D. (2014). The effect of acid accumulation in power-transformer oil on the aging rate of paper insulation. IEEE Electrical Insulation Magazine, 30(3), 19-26. https://doi.org/10.1109/MEI.2014.6804738.

Liimatainen, H., Visanko, M., Sirvio, J. A., Hormi, O. E. O., & Niinimaki, J. (2012). Enhancement of the Nano fibrillation of Wood Cellulose through Sequential Periodate-Chlorite Oxidation. Biomacromolecules, 13(5), 1592-1597. https://doi.org/ 10.1021/bm300319m.

Liimatainen, H., Visanko, M., Sirvio, J. A., Hormi, O. E. O., & Niinimaki, J. (2013). Sulfonated cellulose nanofibrils obtained from wood pulp through regioselective oxidative bisulfite pre-treatment. Cellulose, 20(2), 741-749. https://doi.org/10. 1007/s10570-013-9865-y.

Lindh, J., Carlsson, D. O., Str0mme, M., & Mihranyan, A. (2014). Convenient One-Pot Formation of 2,3-Dialdehyde Cellulose Beads via Periodate Oxidation of Cellulose in Water. Biomacromolecules, 15(5), 1928-1932. https://doi.org/10.1021/bm5002944.

Luo, H.-T., Kang, Y.-R., Nie, H.-Y., & Yang, L.-M. (2009). Sulfamic Acid as a Cost-Effective and Recyclable Catalyst for ^-Amino Carbonyl Compounds Synthesis. Journal of the Chinese Chemical Society, 56(1), 186-195. https://doi.org/10.1002/jccs.200900027.

Maekawa, E. (1991). Analysis of oxidized moiety of partially periodate-oxidized cellulose by NMR spectroscopy. Journal of Applied Polymer Science, 43(3), 417-422. https:// doi.org/10.1002/app.1991.070430301.

Maekawa, E., & Koshijima, T. (1984). Properties of 2,3-dicarboxy cellulose combined with various metallic ions. Journal of Applied Polymer Science, 29(7), 2289-2297. https://doi.org/10.1002/app.1984.070290705.

Munster, L., Capáková, Z., Fišera, M., Kuřitka, I., & Vícha, J. (2019). Biocompatible dialdehyde cellulose/poly(vinyl alcohol) hydrogels with tunable properties. Carbohydrate Polymers, 218, 333-342. https://doi.org/10.1016/j.carbpol.2019.04. 091.

Munster, L., Fojtů, M., Capáková, Z., Vaculovič, T., Tvrdoňová, M., Kuřitka, I., et al. (2019). Selectively oxidized cellulose with adjustable molecular weight for controlled release of platinum anticancer drugs. Biomacromolecules. https://doi.org/10.1021/ acs.biomac.8b01807.

Munster, L., Vícha, J., Klofáč, J., Masař, M., Hurajová, A., & Kuřitka, I. (2018). Dialdehyde cellulose crosslinked poly(vinyl alcohol) hydrogels: Influence of catalyst and crosslinker shelf life. Carbohydrate Polymers, 198, 181-190. https://doi.org/10. 1016/j.carbpol.2018.06.035.

Munster, L., Vícha, J., Klofáč, J., Masař, M., Kucharczyk, P., & Kuřitka, I. (2017). Stability and aging of solubilized dialdehyde cellulose. Cellulose, 24(7), 2753-2766. https:// doi.org/10.1007/s10570-017-1314-x.

Negahdar, L., Delidovich, I., & Palkovits, R. (2016). Aqueous-phase hydrolysis of cellulose and hemicelluloses over molecular acidic catalysts: Insights into the kinetics and reaction mechanism. Applied Catalysis B Environmental, 184, 285-298. https://doi. org/10.1016/j.apcatb.2015.11.039.

Petersen, B. O., Motawie, M. S., M0ller, B. L., Hindsgaul, O., & Meier, S. (2015). NMR characterization of chemically synthesized branched a-dextrin model compounds. CarbohydrateResearch, 403, 149-156. https://doi.org/10.1016/j.carres.2014.05.011.

Rinaldi, R., Meine, N., vom Stein, J., Palkovits, R., & Schuth, F. (2010). Which controls the depolymerization of cellulose in ionic liquids: The solid acid catalyst or cellulose? ChemSusChem, 3(2), 266-276. https://doi.org/10.1002/cssc.200900281.

Rocha, I., Ferraz, N., Mihranyan, A., Str0mme, M., & Lindh, J. (2018). Sulfonated nanocellulose beads as potential immunosorbents. Cellulose, 25(3), 1899-1910. https:// doi.org/10.1007/s10570-018-1661-2.

Ruan, C.h.-Q., Str0mme, M., & Lindh, J. (2018). Preparation of porous 2,3-dialdehyde cellulose beads crosslinked with chitosan and their application in adsorption of Congo red dye. Carbohydrate Polymers, 181, 200-207. https://doi.org/10.1016/]'. carbpol.2017.10.072.

Sarkate, A., Sangshetti, J. N., Dharbale, N. B., Sarkate, A. P., & Shinde, D. B. (2015). Sulfamic acid catalyzed five component reaction for efficient and one-pot synthesis of densely functionalized tetrahydropyridine scaffold. Journal of the Chilean Chemical Society, 60(1), 2832-2836. https://doi.org/10.4067/S0717-97072015000100012.

Shrotri, A., Kobayashi, H., & Fukuoka, A. (2018). Cellulose depolymerization over heterogeneous catalysts. Accounts of Chemical Research, 51(3), 761-768. https://doi.org/ 10.1021/acs.accounts.7b00614.

Sirvio, J. A., Liimatainen, H., Visanko, M., & Niinimaki, J. (2014). Optimization of dicarboxylic acid cellulose synthesis: reaction stoichiometry and role of hypochlorite scavengers. Carbohydrate Polymers, 114, 73-77. https://doi.org/10.1016/jZcarbpol. 2014.07.081.

Spedding, H. (1960). Infrared spectra of periodate-oxidised cellulose. Journal of the Chemical Society (Resumed), 3147-3152. https://doi.org/10.1039/jr9600003147.

Stephens, P. J., Devlin, F. J., Chabalowski, C. F., & Frisch, M. J. (1994). Ab initio calculation of vibrational absorption and circular dichroism spectra using density functional force fields. The Journal of Physical Chemistry, 98(45), 11623-11627. https://doi.org/10.1021/j100096a001.

Suopajarvi, T., Liimatainen, H., Hormi, O., & Niinimaki, J. (2013). Coagulation-flocculation treatment of municipal wastewater based on anionized nanocelluloses. Chemical Engineering Journal, 231, 59-67. https://doi.org/10.1016/jZ cej.2013.07.010.

Tejado, A., Alam, M. N., Antal, M., Yang, H., & van de Ven, T. G. M. (2012). Energy requirements for the disintegration of cellulose fibers into cellulose nanofibers. Cellulose, 19(3), 831-842. https://doi.org/10.1007/s10570-012-9694-4.

Tomasi, J., Mennucci, B., & Cammi, R. (2005). Quantum mechanical continuum solvation models. Chemical Reviews, 105(8), 2999-3094. https://doi.org/10.1021/cr9904009.

Veelaert, S., de Wit, D., Gotlieb, K. F., & Verhé, R. (1997). Chemical and physical transitions of periodate oxidized potato starch in water. Carbohydrate Polymers, 33(2-3), 153-162. https://doi.org/10.1016/S0144-8617(97)00046-5.

Visanko, M., Liimatainen, H., Sirvio, J. A., Haapala, A., Sliz, R., Niinimaki, J., et al. (2014). Porous thin film barrier layers from 2,3-dicarboxylic acid cellulose nanofibrils for membrane structures. Carbohydrate Polymers, 102, 584-589. https://doi.org/ 10.1016/j.carbpol.2013.12.006.

Wagenknecht, W., Nehls, I., & Philipp, B. (1993). Studies on the regioselectivity of cellulose sulfation in an N2O4-N,N-dimethylformamide-cellulose system. Carbohydrate Research, 240, 245-252. https://doi.org/10.1016/0008-6215(93)84187-B.

Yan, G., Zhang, X., Li, M., Zhao, X., Zeng, X., Sun, Y., et al. (2019). Stability of soluble dialdehyde cellulose and the formation of hollow microspheres: Optimization and characterization. ACS Sustainable Chemistry & Engineering, 7(2), 2151-2159. https:// doi.org/10.1021/acssuschemeng.8b04825.

Yang, H., Alam, M. N., & van de Ven, T. G. M. (2013). Highly charged nanocrystalline cellulose and dicarboxylated cellulose from periodate and chlorite oxidized cellulose fibers. Cellulose, 20(4), 1865-1875. https://doi.org/10.1007/s10570-013-9966-7.

Zhang, K., Brendler, E., Geissler, A., & Fischer, S. (2011). Synthesis and spectroscopic analysis of cellulose sulfates with regulable total degrees of substitution and sulfation patterns via 13C NMR and FT Raman spectroscopy. Polymer, 52(1), 26-32. https:// doi.org/10.1016/j.polymer.2010.11.017.